CHEMISTRY
A European Journal

A Journal of
ChemPubSoc Europe

Accepted Article

Title: Reductive Elimination Leading to C-C Bond Formation in Gold(III) Complexes: A Mechanistic and Computational Study

Authors: Manfred Bochmann, Luca Rocchigiani, Julio Fernandez-Cestau, and Peter Budzelaar

To be cited as: *Chem. Eur. J.* 10.1002/chem.201801277

Link to VoR: http://dx.doi.org/10.1002/chem.201801277

Supported by
ACES

WILEY-VCH

10.1002/chem.201801277

WILEY-VCH

Reductive Elimination Leading to C-C Bond Formation in Gold(III) Complexes: A Mechanistic and Computational Study

Luca Rocchigiani,*[a] Julio-Fernandez-Cestau,[a] Peter H. M. Budzelaar*[b] and Manfred Bochmann*[a]

Abstract: The factors affecting the rates of reductive C-C cross-coupling reactions in gold(III) aryls were studied using complexes that allow easy access to a series of electronically modified aryl ligands, as well as to gold methyl and vinyl complexes, using the pincer compounds (C^N^C)AuR (R = C_6F_5, CH=CMe_2, Me and *p*-C_6H_4X, where X = OMe, F, H, Bu^t, Cl, CF_3, or NO_2) as starting materials (C^N^C = 2,6-(4′-$Bu^tC_6H_3$)$_2$pyridine dianion). Protode-auration followed by addition of 1 equiv. SMe_2 leads to the quantitative generation of the thioether complexes [(C^N-CH)-AuR(SMe_2)]$^+$. Upon addition of a second SMe_2 pyridine is displaced, which triggers reductive aryl-R elimination. The rates for these cross-couplings increase in the sequence *k*(vinyl) > *k*(aryl) >> *k*(C_6F_5) > *k*(Me). Vinyl-aryl coupling is particularly fast, 1.15 × 10^{-3} L mol^{-1} s^{-1} at 221 K, while both C_6F_5 and Me couplings encountered higher barriers for the C-C bond forming step. Using P(*p*-tol)$_3$ in place of SMe_2 greatly accelerates C–C couplings. Computational modelling shows that in the C^N bonded compounds displacement of N by a donor L is required before the aryl ligands can adopt a conformation suitable for C-C bond formation, so that elimination takes place from a four-coordinate intermediate. C-C bond formation is rate limiting. In the non-chelating case, reductive C(sp^2)-C(sp^2) elimination from three-coordinate cations [(Ar^1)(Ar^2)AuL]$^+$ is almost barrierless, particularly if L = phosphine.

Introduction

Reductive elimination leading to C-C bond formation constitutes the product-generating step in many transition metal–catalyzed reactions. Given that gold catalysts have in recent years become a major research focus,[1] reductive elimination and C-C bond forming reactions of gold(III) complexes have attracted particular attention.[2] Early pioneering work showed that the reductive elimination of ethane from neutral gold(III) methyl complexes is slow, which explains their thermal stability,[3] but in $Me_2Au(OTf)(H_2O)$ is accelerated when the water ligand is displaced by PPh_3.[4] Cationic dimethyl complexes [Me_2AuL_2]$^+$ were found to eliminate ethane faster than neutral complexes, and the rate of reductive elimination was shown to depend on L in the sequence L = PMe_3 < PMe_2Ph < $PMePh_2$ < PPh_3.[5] Recent computational models showed that methyl-methyl elimination from $Me_2AuCl(PPh_3)$ is kinetically inaccessible due to the directionality of the Au-C bond, which needs to weaken before a compensating C···C bond can develop.[6] On the other hand, Toste and co-workers found that the rate of ethane elimination from [$Me_2Au(PR_3)_2$]$^+$ (R = Me, Et) was enhanced by a factor of up to 10^7 in the presence of catalytic quantities of a supramolecular cage, provided the cage cavity was spacious enough to accommodate the cation. This effect highlights the importance of steric factors in lowering the barrier of reductive eliminations.[7] However, C(sp^3)-C(sp^3) couplings remain generally challenging.

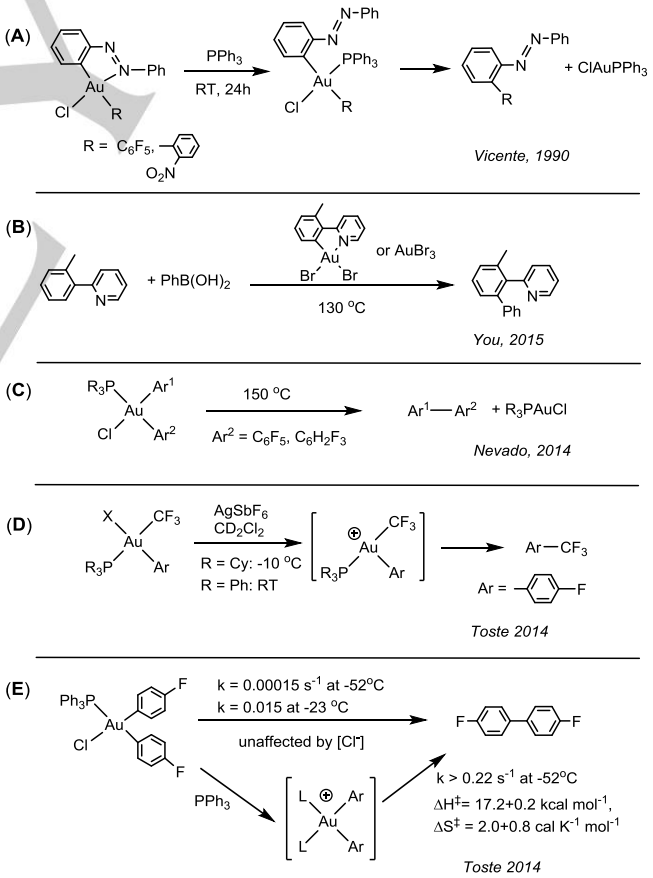

Scheme 1. Illustrations of reductive elimination reactions of gold(III) complexes.[8,9,13,16,17]

[a] Dr. L. Rocchigiani, Dr. J. Fernandez-Cestau, Prof. Dr. M. Bochmann
School of Chemistry, University of East Anglia
Norwich Research Park
NR47TJ, Norwich, UK
E-mail: l.rocchigiani@uea.ac.uk; m.bochmann@uea.ac.uk
[b] Prof. Dr. P. H. M. Budzelaar
Department of Chemistry
University of Naples Federico II
Via Cintia, 80126, Naples, Italy
E-mail: p.budzelaar@unina.it

Supporting information for this article is given via a link at the end of the document.

The reductive elimination leading to aryl-aryl cross-coupling products in cyclometallated C^N chelate gold(III) complexes was first shown by Vicente et al. to be induced by the addition of PPh_3, which was thought to displace the nitrogen donor prior to the $C(sp^2)$-$C(sp^2)$ bond forming step. This reaction proceeds at room temperature (Scheme 1A).[8] More recently, You et al. reported the catalytic *ortho*-arylation of cyclometallating 2-arylpyridines with arylboronic acids using $AuBr_3$ or (C^N)$AuBr_2$ as a catalysts in the presence of an oxidant; this phosphine-free system requires forcing conditions (130 °C, Scheme 1B).[9] On the other hand, *ortho*-substituted and electron-withdrawing aryls, such as mesityl and C_6F_5, give thermally stable, isolable cations $[L_2AuAr_2]^+$ (L = N or P-donor ligand), which in spite of their conformational flexibility are resistant to reductive elimination.[10,11]

The nature of the species involved in catalysis is often speculative, while the range of studies on well-defined complexes is so far limited to specific alkyls or aryls and does not yet allow a general picture to be drawn of the factors that favour reductive elimination. For example, in mechanistic studies on the selective cross-coupling of arenes with arylsilanes to give Ar-Ar′ catalyzed by phosphine-free gold(III) catalysts, intermediates of the general structure (Ar)(Ar′)AuX_2 have been proposed but the nature of X (neutral or anionic ligand) remained undefined.[12]

More precise information about the structure of species involved in reductive elimination is available for phosphine complexes $(R_3P)AuCl(R^1)(R^2)$, where R^1 = aryl and R^2 = either fluoroaryl or CF_3. Nevado showed that the aryl-aryl coupling reactions from neutral gold fluoroaryl complexes require high temperatures (150 °C) and, in the presence of sacrificial oxidants, can be extended to the catalytic direct coupling of *p*-xylene with $C_6F_5B(OH)_2$ (Scheme 1C).[13,14] Variations of the phosphine ligand in similar cross-coupling reactions of perfluoroaryls at 85 – 150 °C showed that the steric requirements of the phosphines seem to play a larger role than their electronic properties.[15] In all these cases elimination was thought to proceed from a four-coordinate phosphine complex.

Much faster elimination rates were found in the otherwise challenging reductive $C(sp^2)$-$C(sp^3)$ coupling of aryls with CF_3, provided the halide ligand was removed with a silver salt, generating a three-coordinate species $[(R_3P)Au(aryl)(CF_3)]^+$. Under these conditions the aryls *p*-C_6H_4X (X = H, F, Me, OMe) all undergo aryl-CF_3 coupling within less than a minute at or below room temperature (Scheme 1D).[16] The reductive aryl-aryl coupling of in-situ generated (and non-isolable) $(Ph_3P)AuClAr^F{}_2$ (Ar^F = *p*-C_6H_4F) proceeds exceptionally rapidly even at -52 °C and, far from being favoured by ligand dissociation and formation of a three-coordinate species, was found to be strongly *accelerated* by the addition of phosphine. It was proposed that under these conditions chloride displacement leads to the formation of $[(Ph_3P)_2AuAr^F{}_2]^+$ cations, which are too unstable to accumulate in detectable concentrations but give very rapid C-C coupling (Scheme 1E).[17] It is entirely possible that even the reductive elimination from the neutral $(Ph_3P)AuClAr^F{}_2$ is preceded by ligand rearrangement to transient $[(Ph_3P)_2AuAr^F{}_2]^+$, such that the measured rate refers to that rearrangement and not to the actual C-C coupling step. However, C_6H_4F appeared to be an "exceptionally fast" case, and this reaction was not extended to other aryls. Computational modelling of this reaction proposed a contribution of heavy-atom tunneling to the bond formation rates in the system $(Ph_3P)AuCl(R^1)(R^2)$ and suggested that the rate of aryl-aryl coupling in $[(Ph_3P)_2AuAr^F{}_2]^+$ should be 10^4 times faster than was actually observed.[6]

It is evident therefore that the rates of C-C coupling reactions in gold(III) complexes are subject to strong ligand effects, with both three-coordinate and four-coordinate transition states likely involved. Even isostructural cationic systems $[L_2AuR_2]^+$ show behavior ranging from high thermal stability to extremely rapid reductive elimination, with rates varying as a function of L and R by many orders of magnitude. In an effort to elucidate the factors governing reductive C-C bond forming reactions in gold(III) systems, we were looking for a system which gave easy access to a wide range of aryl, alkyl and alkenyl complexes and which would react at comparable rates for all types of C-ligands, in a range suitable for monitoring by NMR spectroscopy. We therefore concentrated on (C^N^C)Au-R pincer complexes,[18-22] since these compounds are synthetically readily accessible and reductive elimination can easily be induced by a protocol involving protolytic cleavage of one pincer Au-C bond,[22,23] followed by addition of a donor ligand L (Scheme 2). We report here the mechanism of reductive aryl–R coupling, where R = aryl, vinyl or methyl, together with the identification of the role of donor ligands and computational modelling of these reaction sequences.

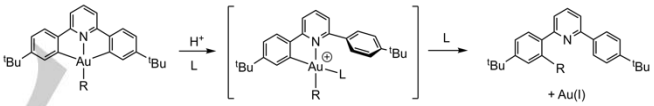

Scheme 2. General pathway for reductive aryl-R elimination in gold(III) complexes.

Results and Discussion

Reductive Eliminations induced by SMe_2

The complexes (C^N^C)$AuAr^x$ **1a** – **1g** (Ar^x = *p*-C_6H_4X, where X = **a**, OMe; **b**, F; **c**, H; **d**, Bu^t; **e**, Cl; **f**, CF_3; **g**, NO_2) were synthesized by heating (C^N^C)AuOH in toluene with the corresponding boronic acids in good yields (C^N^C = 2,6-(4′-$Bu^tC_6H_3$)$_2$pyridine dianion). The electronic effect of the *para*-substituent X is evident from the ^{13}C NMR shifts of the Au–C(Ar^x) atom in **1** and increases linearly with the σ_P parameter of X = OMe (δ_C = 138.2), H (147.8) and NO_2 (158.6 ppm).

C(aryl)-C(C_6H_4X) Reductive Elimination. Although reductive eliminations are most frequently induced by phosphine ligands, we found that SMe_2 plays the same role but is less subject to steric factors and gives reaction rates that can be conveniently followed by NMR spectroscopy. Preliminary tests showed that the reaction of (C^N^C)$AuAr^{OMe}$ with the strong solid Brønsted acid $[H(OEt_2)_2][H_2N\{B(C_6F_5)_3\}_2]$[24] ($HAB_2$) at room temperature leads to the quantitative generation of the protodeauration

product $[(C^N\text{-}CH)Au(Ar^{OMe})(OEt_2)]^+$, which is stable towards C-C coupling over a period of several hours. The addition of 1 molar equivalent of SMe_2 displaced the ether ligand to give $[(C^N\text{-}CH)Au(Ar^{OMe})(SMe_2)]^+$ (**2a**), which is thermally sufficiently stable in CD_2Cl_2 solution to be characterized by NMR spectroscopy. Heating this solution to reflux for 5 minutes triggered reductive elimination and quantitative formation of the cross-coupling product **3a**. On the other hand, the addition of 5 equivalents of SMe_2 to **2a** at the same temperature induced immediate reductive elimination, which was too fast at room temperature to follow the kinetics. It is evident that the addition of the first SMe_2 molecule leads to a resting state, and a second SMe_2 is required to trigger fast reductive elimination. This implies substitution of the pyridine donor, which enables the geometric flexibility required to reach the coupling transition state (Scheme 3). This scenario resembles that observed by Vicente *et al*. for the action of PPh_3 on (C^N)gold chelates (Scheme 1A).[8] The high reactivity of gold(III) aryls $[(Me_2S)_2Au(Ar^1)(Ar^2)]^+$ is in sharp contrast with the thermal stability of the platinum analogues $(Me_2S)_2PtR_2$ (R = Ph, *p*-tol), which undergo substitution of the SMe_2 ligands but no reductive C-C coupling.[25]

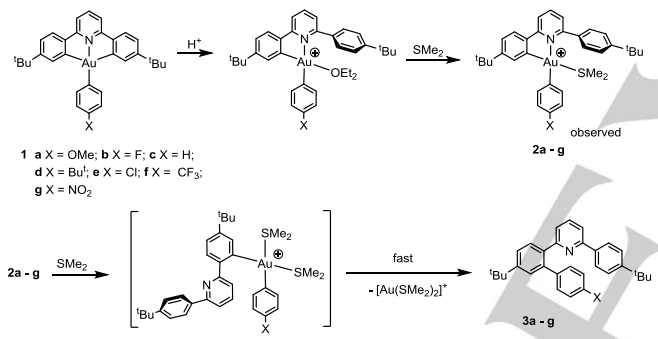

Scheme 3. SMe_2 induced $C(sp^2)$-$C(sp^2)$ reductive elimination in bis(aryl)-gold(III) cations.

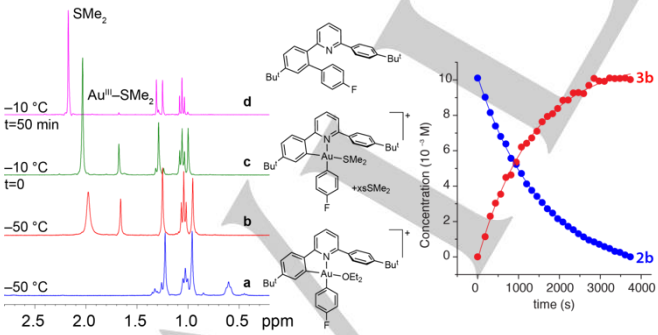

Figure 1. Left: Evolution of the aliphatic region of the ^1H NMR spectrum of $[(C^N\text{-}CH)Au(Ar^{OMe})(OEt_2)]^+$ (a), after addition of 4 SMe_2 at –50 °C (b), and upon raising the temperature to –10 °C (c, d) (CD_2Cl_2). Right: Kinetics of the conversion of **2b** into **3b** at -10 °C.

Protodeauration of the *p*-fluorophenyl complex **1b** at 25 °C, followed by addition of four molar equivalents of SMe_2 at -50 °C showed that at this temperature only the adduct $[(C^N\text{-}CH)Au(Ar^F)(SMe_2)]^+$ (**2b**) was formed, in spite of the presence of excess SMe_2. On raising the temperature to -10 °C reductive elimination was observed, and **2b** was converted into **3b** over a period of about 1 hour (Figure 1).

Reactant decay and product formation are monoexponential under these conditions. Given that coordination of the first SMe_2 leads to a resting state and the second molecule of SMe_2 triggers C-C coupling, a second-order rate law can be assumed, $-d[Au]/dt = k[Au][SMe_2]$ (where Au = $[(C^N\text{-}CH)Au\text{-}R(SMe_2)]^+$). Experiments at three different SMe_2 concentrations gave an average $k = 1.17 \times 10^{-2}$ L mol^{-1} s^{-1} (CD_2Cl_2, -10 °C).

Table 1. Kinetic data for the reductive elimination from protodeaurated pincer complexes in CD_2Cl_2.

$[Au]_0$ (mM)	T (K)	$[SMe_2]$	k_2 (L mol^{-1} s^{-1})	k_{2av} (L mol^{-1} s^{-1})
2a (C_6H_4OMe)				
12.5	263	70.2	4.32×10^{-2}	$5.8\pm1.5\times10^{-2}$
14.2		80.3	7.34×10^{-2}	
12.1		75.6	5.64×10^{-2}	
2b (C_6H_4F)				
13.5	263	57.1	1.23×10^{-2}	$1.2\pm0.1\times10^{-2}$
13.3		53.2	1.12×10^{-2}	
16.1		89.6	1.14×10^{-2}	
2c (C_6H_5)				
19.1	263	91.6	2.37×10^{-2}	$2.2\pm0.2\times10^{-2}$
14.6		100.2	2.02×10^{-2}	
15.0		105.2	2.33×10^{-2}	
2d ($C_6H_4Bu^t$)				
16.5	263	88.0	3.47×10^{-2}	$3.5\pm0.1\times10^{-2}$
16.2		111.1	3.21×10^{-2}	
15.1		75.6	3.36×10^{-2}	
2e (C_6H_4Cl)				
14.0	263	154.81	1.78×10^{-2}	$1.9\pm0.1\times10^{-2}$
15.0		84.1	1.85×10^{-2}	
9.1		94.3	2.05×10^{-2}	
2f ($C_6H_4CF_3$)				
13.3	263	84.1	1.87×10^{-2}	$1.6\pm0.2\times10^{-2}$
13.1		54.7	1.59×10^{-2}	
15.5		271.6	1.44×10^{-2}	
2g ($C_6H_4NO_2$)				
14.8	263	66.4	4.10×10^{-2}	$3.5\pm0.6\times10^{-2}$
13.6		99.7	2.90×10^{-2}	
16.7		103.9	3.62×10^{-2}	
2h (C_6F_5)				
18.8	298	350.0	-	$1.5\pm0.1\times10^{-3}$
2i ($CH{=}CMe_2$)				
12.3	221	199.0	-	$1.2\pm0.1\times10^{-3}$
2j (Me)				
13.2	298	214.7	-	$3.8\pm0.3\times10^{-6}$

The complexes **1c** – **1g** react similarly to give intermediates and C–C coupling products that were characterized by $^1H/^{13}C$ NMR (Experimental Section). The reaction rates were measured

at -10 °C in CD_2Cl_2 and the results of the data interpolation are reported in Table 1. All the reactions show very similar second-order rate constants, of the order of 10^{-2} L mol^{-1} s^{-1}, which means that the electron donating or withdrawing character of X does not have a significant effect on the apparent rate of C–C coupling.

The Hammett plot of the Au-C_6H_4X derivatives as a function of the σ_P parameter (Figure 2) shows a V-shaped correlation with very moderate ρ values of –1.8 (left) and 0.5 (right). There is a linear decrease in rates going from electron-donating to electron-withdrawing substituents in the series from X = OMe to X = F, although rates increase again for X = NO_2. The mechanistic reason for this variation has been explored by computational modelling (vide infra), although its origins proved difficult to pinpoint. In any case, the effect of aryl *p*-substituents is small compared to the differences in rates when the aryl ring is changed to C_6F_5, vinyl or methyl.

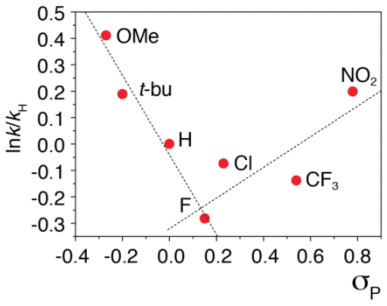

Figure 2. Correlation of reductive elimination rates of p-substituted gold(III) aryls 2a – g with the Hammett parameter σP.

Aryl-C_6F_5, Aryl-Vinyl and Aryl-Methyl Reductive Eliminations. In order to extend the study, the same HAB_2 / SMe_2 elimination protocol was applied to (C^N^C)AuC_6F_5 (**1h**). Contrary to what was observed with the other aryl species, the protodeaurated complex [(C^N-CH)Au(C_6F_5)(SMe_2)]$^+$ (**2h**) is a rather stable product, even in the presence of 20 equivalents of SMe_2. Monitoring the reaction over the course of several days shows that slow reductive elimination does take place, to give **3g** (Scheme 4). At 25 °C the reaction is complete after 7 days, leading to a rate constant of 1.5 × 10^{-5} L mol^{-1} s^{-1}. Considering that the reaction of the other aryls are too fast to be followed at room temperature and extrapolation from -10 °C gives a minimum k > 1 s^{-1} for the formation of **3a** – **3g**, the reaction leading to **3h** is about five orders of magnitude slower.

The opposite rate trend was found for C(sp^2)-C(sp^2) cross-couplings where one coupling partner was a vinyl ligand. Gold vinyl species constitute an important class of C(sp^2) groups; they are intermediates in nucleophilic activation of alkynes, and subsequent C-C bond formations of gold vinyls have been extensively incorporated into synthetic methodology.[1g,1k] To investigate Au-vinyl reactivity, we targeted (C^N^C)AuCH=CMe_2 (**1i**), which was obtained in good yield by reacting (C^N^C)AuCl with BrMgCH=CMe_2 in THF. Protonation of **1i** with HAB_2 in CD_2Cl_2 at -10 °C followed by addition of 12 equivalents of SMe_2 caused instantaneous reductive elimination of **3i**, an indication that vinyls react significantly faster than aryls.

At -52 °C the reaction is slow enough for the kinetics to be followed by ^{1}H NMR spectroscopy. Assuming the same second-order rate law as for aryls, a rate constant k = 1.15 × 10^{-3} L mol^{-1} s^{-1} (at 221 K) was obtained. This compares with the rate of reductive elimination of 4,4'-difluorobiphenyl from PPh_3AuCl(Ph^F)$_2$ plus PPh_3 (0.019 L mol^{-1} s^{-1}).[17] Most likely, our process is still slower than the latter because the pyridine displacement by SMe_2 is slower than the chloride displacement in (Ph_3P)AuCl(Ph^F)$_2$ by PPh_3.

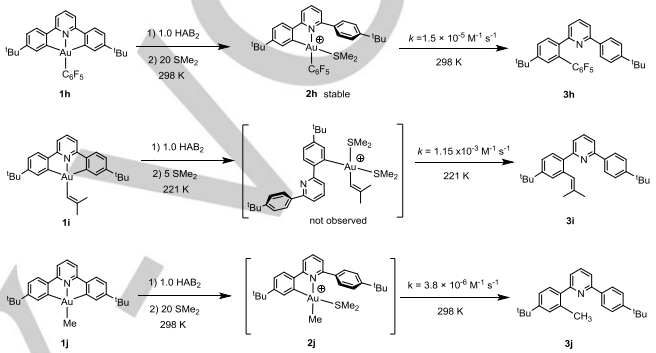

Scheme 4. SMe_2-induced aryl-C_6F_5, aryl-vinyl and aryl-methyl reductive elimination reactions.

Cross-coupling reactions involving sp^3-carbon are most challenging. Protodeauration of (C^N^C)AuMe[22] (**1j**) with HAB_2 in CD_2Cl_2 gave [(C^N-CH)AuMe(OEt_2)]$^+$ which is stable in solution at room temperature for several days. As was the case with the Au-C_6F_5 complex, adding an excess of SMe_2 replaced the ether but did not induce further reaction. Reductive elimination occurred only very slowly over the course of weeks, to give the methyl-substituted arene **3j**, with an estimated rate constant of 3.8 × 10^{-6} L mol^{-1} s^{-1}, about one order of magnitude slower than the pentafluorophenyl complex. The rates of SMe_2-induced reductive C-C cross-coupling reactions in these gold(III) aryls therefore decrease in the order

$$k(\text{vinyl}) > k(\text{aryl}) >> k(C_6F_5) > k(\text{Me})$$

Reductive elimination in pyrazine-based C^N^{pz}^C complexes. The results obtained so far with C^N^C complexes of type **1** indicated that the barrier for C–C coupling likely involved pyridine displacement. Pyrazine is about five orders of magnitude less basic than pyridine.[26] It was therefore of interest to compare the reductive elimination process of C^N^{py}^C complexes **1** with the analogous pyrazine compounds (C^N^{pz}^C)Au(aryl) **4**,[27] which could be expected to be substitutionally more labile.

(C^N^{pz}^C)Au(*p*-C_6H_4OMe) **4a** was be obtained from the reaction of (C^N^{pz}^C)AuOAc^F and *p*-$MeOC_6H_4B(OH)_2$ (OAc^F = trifluoroacetate). Protonation of **4a** can occur on two sites, the Au-C bond and the uncoordinated pyrazine-N atom. Unfortunately, the reaction of **4a** with 1 equivalent of [H(OEt_2)$_2$][AB_2] at room temperature gave a broad and

unresolved ^{1}H NMR spectrum, hampering the characterization of the reaction mixture. Nevertheless, addition of SMe_2 to this solution produced very cleanly the reductive elimination product **6a**. Even at -10 °C the formation of **6a** was too fast to be monitored by ^{1}H NMR spectroscopy, while at -52 °C only the expected deep-red protonated species **5a** was seen (Scheme 5). On the other hand, if protonation is carried out at room temperature followed by cooling to -52 °C and addition of SMe_2 at that temperature, reductive elimination was observed immediately, without any induction period. Under these conditions the apparent rate of reductive elimination is significantly faster than with the pyridine system, and faster than the rate reported previously[17] for $[(Ph_3P)_2Au(C_6H_4F)_2]^+$ complexes. Because of the broadness of the NMR signals, the possibility cannot be excluded that reductive elimination already takes place on protonation, even before SMe_2 is added, with the non-coordinated N-atom of pyrazine acting as donor. Whatever the precise pathway, it is clear that under identical protocols the pyrazine complexes give substantially faster reductive C-C coupling than their pyridine analogues.

In order to get a better understanding of the protonation process, we investigated the reactivity of (C^N^{pz}^C)AuCl **7**, which cannot give reductive elimination. The ^{1}H NMR spectrum obtained upon mixing **7** with HAB_2 (molar ratio 1:1) suggests the formation of the binuclear complex **8**, in which a neutral pyrazine complex stabilizes a cationic Au-C cleavage product by N-coordination (Scheme 5). As NMR diffusion measurements show, the two sets of signals diffuse together and show mutual NOE interactions. Complex **8** appears fairly stable and does not react with a second equivalent of HAB_2. The addition of SMe_2 cleanly generates one single species, which on the basis of NMR studies (diffusion, NOE, VT) was identified as the bis-SMe_2 adduct **9**. Translating the formation of **9** to gold aryl complexes, it seems likely that **9** closely resembles the species that immediately precedes the C-C coupling reaction.

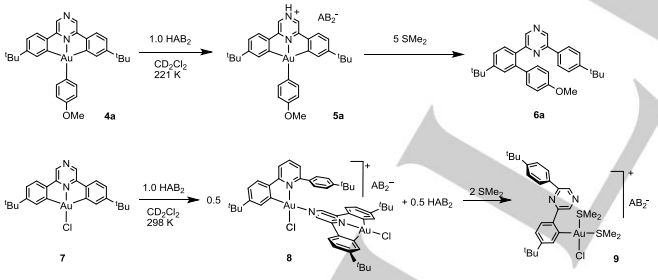

Scheme 5. Reactions of pyrazine-based gold complexes.

Reductive Elimination induced by P(p-tol)$_3$.

The results for complexes of type **1** discussed above serve to show that the rate of reductive C–C coupling is affected by the rate of displacement of the pyridine ligand by SMe_2. If the pyridine is not displaced, C-C reductive elimination does not take place. For comparison with SMe_2, and in order to relate these reactions to those reported previously for gold phosphine complexes (Scheme 1), experiments were carried out with tris(*p*-tolyl)phosphine as donor ligand. P(*p*-tol)$_3$ is not only more coordinating than SMe_2, it is also sterically more demanding, and this has consequences for the types of reaction intermediates that are generated.

Unlike the reaction with SMe_2, adding 1 molar equivalent of P(*p*-tol)$_3$ to $[(C^N\text{-}CH)Au(C_6H_4F)(OEt_2)]^+$ at room temperature generated not one species but a mixture, which contains no free phosphine. The composition of this mixture could not be determined but plausibly includes the species shown in Scheme 6. There was however no formation of the product of reductive elimination **3b**, which implies that, like SMe_2, adding one equivalent of phosphine does not trigger fast C-C bond formation. Eventually reductive elimination happens very slowly, consistent with a low equilibrium concentration of a bis-phosphine precursor species for C-C coupling.

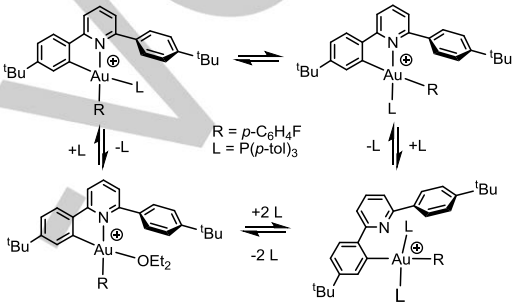

Scheme 6. Possible equilibria on addition of 1.0 equivalents of P(*p*-tol)$_3$ to $[(C^N\text{-}CH)Au(p\text{-}C_6H_4F)(OEt_2)]^+$.

However, over a period of several days, this mixture converted into a single species. Analysis of the 2D NMR spectra showed that reductive elimination had finally occurred and that the product contained an $[AuP(p\text{-}tol)_3]^+$ cation bound to the pyridine. The py-bound gold(I) is released on addition of a second equivalent of phosphine.

On the other hand, treatment of $[(C^N\text{-}CH)Au(C_6H_4F)(OEt_2)]^+$ with *two* equivalents of phosphine from the beginning gives instantaneous reductive elimination at room temperature; no intermediates were observed. The second equivalent of phosphine has the effect of speeding up the reductive elimination step from days to seconds. At -52 °C, on the other hand, the addition of two equivalents of phosphine leads to quantitative formation of the mono-phosphine adduct $[(C^N\text{-}CH)\text{-}Au(C_6H_4F)(Ptol_3)]^+$ **10b** (δ_P = 31.3), leaving 1 equivalent of free P(*p*-tol)$_3$, with no trace of reductive elimination (Scheme 7). Evidently, at that temperature, coordination to pyridine is preferred to a second phosphine. The methyl groups of P(*p*-tol)$_3$ appear as two signals in 2:1 ratio, indicative of hindered rotation. Two isomers are possible for **10b**, with P either *cis* or *trans* to C. Calculations showed that both isomers are of almost equal energy, possibly due to competition between steric bulk and *trans* effect, with P *trans* to C being marginally more stable by 1.6 kcal/mol. Upon warming solutions of **10b** to temperatures above -20 °C reductive elimination occurs very fast to give C–C coupling; intermediates such as $[(C\text{-}N\text{-}CH)Au(C_6H_4F)(Ptol_3)_2]^+$ were not detected.

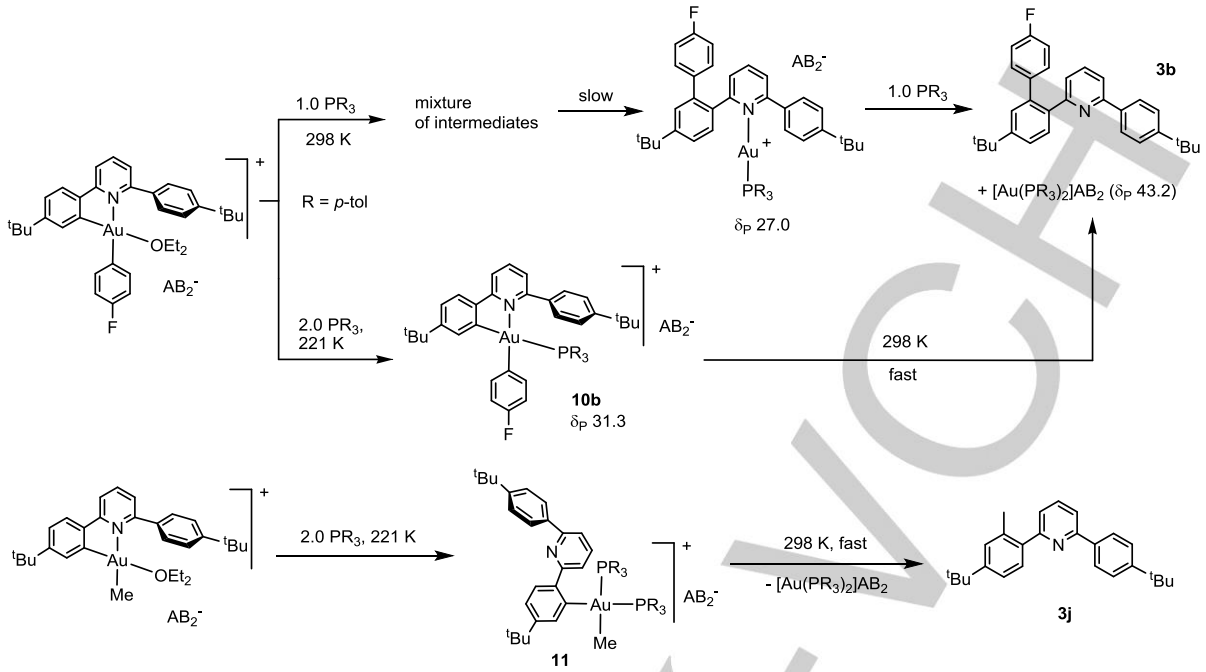

Scheme 7. Phosphine-initiated reductive C-C cross-coupling reactions, including proposed reaction intermediates (R = *p*-tolyl).

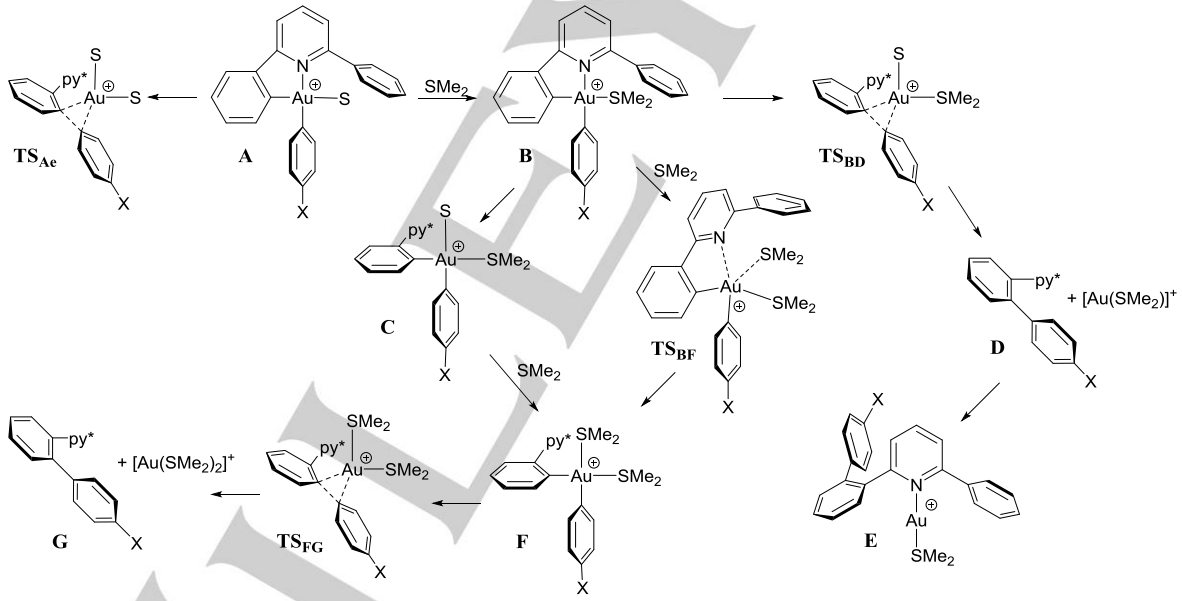

Scheme 8. Pathways for SMe_2-triggered aryl-aryl coupling reactions (S = solvent).

However, for Au-Me complexes bis-phosphine intermediates of type $[(Ar_3P)_2AuR^1R^2]^+$ *do* become observable. Treating the methylgold complex $[(C^N\text{-}CH)AuMe(OEt_2)]^+$ with 2 equivalents of P(*p*-tol)$_3$ at -52 °C gives the bis(phosphine) adduct **11** (Scheme 7), indicated by *(i)* the appearance of two ^{31}P doublets at δ_P 27.5 and 26.0 ($^2J_{PP}$ = 15.0 Hz), *(ii)* diffusion NMR which

shows no free phosphine, *(iii)* a dipolar NOE interaction between the Au–Me resonance and only *one* set of phosphine-aryl signals, and *(iv)* ^{1}H NMR signals around 8 ppm for free rather than coordinated pyridine. As was the case for **10b**, intermediate **11** is thermally unstable, and on warming to room temperature reductive elimination was observed within minutes. Evidently P(*p*-tol)$_3$ induces C(sp^2)-C(sp^3) reductive elimination orders of magnitude faster than SMe_2.

Computational Modelling.

We turned to density functional calculations in order to (a) help understand the observed trends and (b) check to what extent the results for the C^N-CH ligand can be extrapolated to more general organogold(III) chemistry.

Computational studies were done for a model C^N^C ligand lacking the ^{t}Bu substituents at the phenyl rings, using Gaussian 09.[28] Geometries were optimized at the B3LYP[29]/SVP[30] level (LANL2DZ with corresponding ECP at Au[31]) including a PCM(dichloromethane) solvent correction.[32] The nature of stationary points was checked by vibrational analyses. Improved single-point energies were obtained with the TPSSH[33] functional and the cc-pVTZ basis set[34] (and using the corresponding ECP at Au[35]), again including a PCM(dichloromethane) correction. These were combined with a DFT-D3 dispersion correction[36] (zero damping) and with the thermal corrections (enthalpy and entropy) at 298 K, obtained from the B3LYP/SVP vibrational analyses. All energies mentioned are Gibbs free energies.

Reaction path. Elimination paths involving zero, one or two SMe_2 ligands per gold atom were studied for the parent system [(C^N-CH)Au(Ph)]$^+$ (**A**), where the ^{t}Bu groups of (C^N^C)AuPh (**1c**) were omitted from the model. The reactions are summarized in Scheme 8, and Scheme 9 shows the corresponding free energy profile. The structures of a few key transition states are presented in Figure 3.

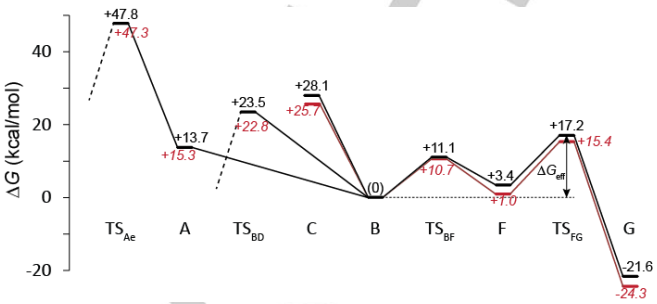

Scheme 9. Free energy profile for SMe_2 assisted reductive elimination from [(C^N-CH)AuPh]$^+$ (**A**). In red and *italics* the corresponding values for pyrazine analogue **A'**.

Unassisted reductive elimination from **A** via **TS$_{Ae}$** , i.e. pyridine substitution by solvent, has a prohibitively high calculated barrier of 34.1 kcal/mol, in line with the observation that **2c** is stable in solution. The main reason for this large barrier is that coordination of the pyridine donor cannot be maintained during the elimination; this is not a general feature of three-coordinate Au species as will become clear later on.

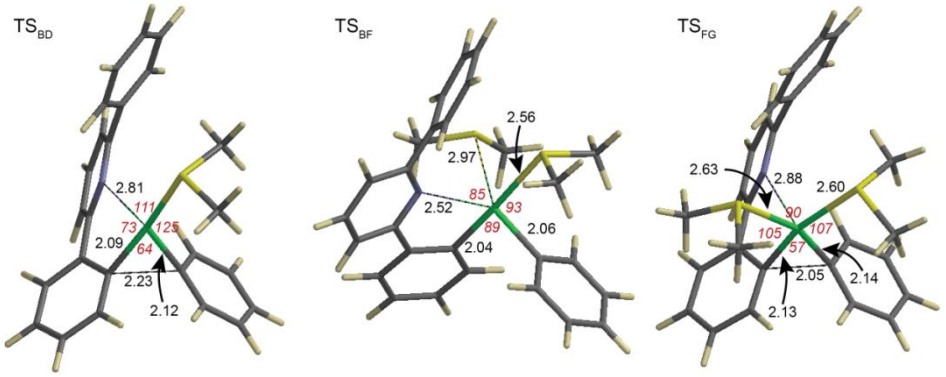

Figure 3. Structures of key transition states on the reductive elimination path (distances in Å, angles in italics).

Coordination of one SMe_2 ligand in the empty "pocket" of **A** to give **B** is exergonic by 13.7 kcal/mol and presumably has a low barrier. There is some steric crowding caused by the dangling CH arm of the C^N-CH ligand, resulting in nonplanarity of the complex, but SMe_2 is a small donor that fits fairly well into the pocket. Reductive elimination from **B** via **TS$_{BD}$** (Figure 3) has a smaller but still sizeable barrier of 23.5 kcal/mol, corresponding to a reaction that is not very fast at room temperature, in agreement with the observation of **2c** by NMR.

The four-coordinate complex **B** is coordinatively saturated and does not bind a fifth ligand. A fully dissociative path for binding of the second SMe_2 molecule is high in energy (via **C**, 28.1 kcal/mol) and not compatible with observed reactivity. However, we were able to locate transition state $\mathbf{TS_{BF}}$ (Figure 3) for concerted displacement of pyridine by an incoming SMe_2 ligand. It features elongated Au-N (2.52 Å) and Au-S (2.97 Å) bonds as expected, and an N-Au-S angle of 85°, indicating an S_N2-retention type mechanism. The barrier for this displacement is low (11.1 kcal/mol), so this would be a fast pre-equilibrium at room temperature. However, the displacement is slightly endergonic (3.4 kcal/mol), so one would not expect the bis(thioether) complex **F** to be observable by NMR. From **F**, the barrier for C-C coupling via $\mathbf{TS_{FG}}$ is only 13.8 kcal/mol. Since **B** is the resting state for this thioether-induced coupling, the effective barrier (that would correspond to experimental kinetics[37]) is 17.2 kcal/mol, consisting of a contribution from py displacement (**B**→**F**, 3.4 kcal/mol) and the subsequent elimination (**F**→$\mathbf{TS_{FG}}$, 13.8 kcal/mol). Based on the energy profile, this would be the rate-limiting step for the preferred elimination path in the presence of excess SMe_2, and the calculated barrier is compatible with a reaction that can be "frozen out" by cooling.

The whole profile was recalculated for the pyrazine analogue **A'** of **A** (see Scheme 8). Differences are found to be modest. Pyrazine is more weakly coordinating, which results in more exergonic binding of the first SMe_2 (**A'**→**B'**, -15.3 vs -13.7 kcal/mol), less endergonic binding of the second one (**B'**→**F'**, 1.0 vs 3.4 kcal/mol) and a slightly lower effective elimination barrier (**B'**→$\mathbf{TS_{F'G'}}$, 15.4 vs 17.2 kcal/mol). Easier elimination is in qualitative agreement with experiment.

Substituent effects. To analyze substituent effects in more detail, we used simplified model systems that don't feature "dangling aryl arms": $[(C^N)Au(Ar)SMe_2]^+$ to study pyridine displacement, and $[(Ph)Au(Ar)(SMe_2)_n]^+$ (n = 1, 2) to study reductive elimination. The ligand Ar was varied over the set of substituents studied experimentally: Ar = *p*-C_6H_4X (X = OMe, ^{t}Bu, H, F, Cl, CF_3, NO_2), C_6F_5, Me and CH=CMe_2 ("Vin"). The results are summarized in Table 3.

Pyridine displacement in the C^N complexes has a higher barrier (by 5.5 kcal/mol for X = H) and is more endergonic (by 4.7 kcal/mol) than for the C^N-CH complex, presumably due to the crowding caused by the dangling -CH arm weakening the Au-py bond. The calculated displacement barriers for X = OMe to X = NO_2 do not vary by much (spread of 1.1 kcal/mol) but show an almost perfect *anti*-correlation with the experimental relative barriers, indicating that py displacement is unlikely to be rate-limiting. The methyl complex has a clearly lower barrier than all C(sp^2) type substituents.

Reductive elimination from three-coordinate $[(Ph)Au(Ar)SMe_2]^+$ is remarkably facile, having a barrier <6 kcal/mol for all Ar groups studied. Inspection of the geometries (see SI, Figures S27 – S29) shows that these eliminations have very early transition states. Such complexes are expected to eliminate instantaneously and would not be isolable. There is hardly any variation in the OMe - NO_2 series (all ~ 3 kcal/mol); C_6F_5 and Vin couple more easily (~ 1.8 kcal/mol) while Me has the highest barrier (5.7 kcal/mol).

Table 3. Substituent effects on displacement and elimination barriers (L = SMe_2).

Ar	py displacement [a]		Elimination [b]		Binding energy [c]
	$\Delta G^{\ddagger}$	ΔG	$(Ph)Au(Ar)L^+$	$(Ph)Au(Ar)L_2^+$	2nd L
C_6H_4OMe	17.70	10.66	2.72	11.88	-17.20
C_6H_4tBu	16.94	9.57	3.16	12.31	-16.50
C_6H_5	16.57	9.00	3.17	13.39	-17.08
C_6H_4F	16.73	8.12	3.19	13.26	-17.83
C_6H_4Cl	16.77	8.70	3.24	13.22	-18.08
$C_6H_4CF_3$	17.00	8.41	3.13	13.27	-18.79
$C_6H_4NO_2$	16.81	8.74	3.50	12.36	-18.22
C_6F_5	16.00	10.19	1.85	16.27	-24.46
Me	14.39	9.83	5.73	21.67	-16.25
Vin	17.13	10.80	1.72	10.17	-15.52

[a] Displacement of the coordinated py group in $[(C^N)Au(Ar)SMe_2]^+$ by SMe_2. [b] Reductive elimination from $[(Ph)Au(Ar)SMe_2]^+$ or $[(Ph)Au(Ar)(SMe_2)_2]^+$. [c] Energy change for $[(Ph)Au(Ar)SMe_2]^+ + SMe_2 \rightarrow [(Ph)Au(Ar)(SMe_2)_2]^+$.

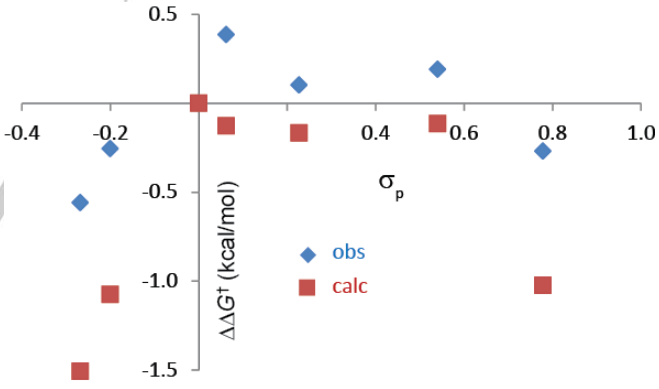

Figure 4. Relative (*vs* H) free energy barriers $\Delta\Delta G^{\ddagger}$ for reductive elimination *vs*. substituent Hammett σ_p: calculated (■) for $[(Ph)Au(Ar)(SMe_2)_2]^+$ and observed (♦) for $[(C^N\text{-}CH)Au(p\text{-}C_6H_4X)]^+$ in the presence of SMe_2.

In the presence of an excess of SMe_2, formation of the bis(thioether) complex $[(Ph)Au(Ar)(SMe_2)_2]^+$ would be essentially quantitative, with a binding energy of ~ -17 kcal/mol (more for C_6F_5, less for Me and Vin). The barriers for elimination from these four-coordinate complexes are ~ 13 kcal/mol, i.e. substantially higher than from the three-coordinate complexes, and the transition states are later (see the SI). Nevertheless, the non-dissociative path is preferred: the effective barrier for the dissociative path $[(Ph)Au(Ar)(SMe_2)_2]^+ \rightarrow ([(Ph)Au(Ar)SMe_2]^+ +$

SMe_2 is ~ 21 kcal/mol, of which ~18 kcal/mol comes from dissociation and 3 kcal/mol from the actual coupling barrier. Substituent effects for the *p*-substituted phenyl groups (X = OMe to NO_2) are modest (11.9 - 13.4 kcal/mol), but the fair agreement between calculated and experimental relative barriers (Figure 4) supports the assignment of the actual C-C coupling step as the rate-limiting step also for the C^N-CH systems. Here, elimination of C_6F_5 has a larger barrier than the *p*-substituted phenyls (16.3 kcal/mol) and methyl-aryl coupling is much more difficult still (21.7 kcal/mol). On the other hand, coupling to Vin is easier (10.2 kcal/mol) than to aryl groups. These results match well with the experimental observations.

The predicted extremely easy C-C coupling in three-coordinate $[(Ph)Au(Ph)SMe_2]^+$ of 3.2 kcal/mol agrees with computational results by Datta[6] for neutral three-coordinate complexes, but contrasts sharply with the prohibitive coupling barrier in corresponding three-coordinate complex **A** ($[(C^N-CH)Au(Ph)]^+$, 34.1 kcal/mol). This is not caused by the different nature of the third ligand (py vs SMe_2) but rather by the geometric constraints imposed by the C^N-CH ligand backbone, which force a loss of most of the py coordination before C-C coupling can begin. To a somewhat smaller degree, the same applies to elimination from $[(Ph)Au(Ph)SMe_2]^+$ (13.4 kcal/mol) vs $[(C^N-CH)Au(Ph)SMe_2]^+$ (23.5 kcal/mol). It is only in the *bis*(thioether) complexes that these geometric effects are lost and $[(C^N-CH)Au(Ph)(SMe_2)_2]^+$ starts behaving like a "normal" four-coordinate complex. Thus, the constraints imposed by the C^N-CH ligand backbone are essential in stabilizing the bis(aryl) complexes against reductive elimination: ligand addition here *facilitates* reductive elimination, in an inversion of the normal stability order.

Phosphine ligands. C-C coupling is more usually associated with phosphine ligands. Evaluation of the whole reaction path including one or two complete $P(p\text{-tol})_3$ ligands was not feasible because of size and conformational issues, so we restricted ourselves to evaluation of the binding of $P(p\text{-tol})_3$ in the "in-pocket" (IP, *cis* to py) and "out-of-pocket" (OP, *trans* to py) coordination sites of **A** (Scheme 8). $P(p\text{-tol})_3$ does not fit comfortably in the limited space of the IP site, but coordination at the OP site requires the formation of an unfavourable *trans* Ar-Au-Ar arrangement. At the level of theory used here, for $[(C^N-CH)Au(p\text{-}C_6H_4F)]^+$, the two effects mostly cancel, leaving a 3.2 kcal/mol preference for the IP site (which reduces to 1.6 kcal/mol when the ligand ^{t}Bu groups are included in the modelling). We conclude that these isomers are close in energy and could both be components of the mixture of intermediates mentioned in Scheme 6.

Beyond this, we used PMe_3 as a generic phosphine model. Since this has very different steric properties we did not attempt to model ligand displacement, and instead concentrated on Au-L bond strength and reductive elimination. Results are summarized in Table 4. PMe_3 binds more strongly than SMe_2 in comparable situations, by about 11-13 kcal/mol. The C-C coupling barriers are rather similar for corresponding PMe_3 and SMe_2 complexes. In particular, the extremely low barrier for elimination from a three-coordinate complex is also seen for this phosphine ligand.

Table 4. Comparison of SMe_2 and PMe_3 behaviour in Ph-Ph reductive elimination

Reaction	SMe_2	PMe_3
L-Au Binding [a]		
A→B	-13.71	-24.78
B→F	3.43	-9.51
$[LAuPh_2]^+ \rightarrow [L_2AuPh_2]^+$	-17.08	-28.08
Elimination [a]		
$B \rightarrow TS_{BD}$	23.48	20.03
$F \rightarrow TS_{FG}$	13.79	15.27
$\Delta G^{\ddagger}$, $[LAuPh_2]^+$	3.17	1.01
$\Delta G^{\ddagger}$, $[L_2AuPh_2]^+$	13.39	14.67

[a] Free energies of SMe_2/PMe_3 binding and free energy barriers for C-C reductive elimination, in kcal/mol.

Conclusions

Reductive C-C cross-coupling reactions can be induced in (C^N^C)AuR pincer complexes by a protocol involving Au-C cleavage by H^+ followed by the addition of a donor L. While no reaction takes place if L = OEt_2, C-C coupling is induced by stronger donors such as L = SMe_2 and $P(p\text{-tol})_3$. The intermediates $[(C^N-CH)ArR(L)]^+$ proved to be observable, thermally comparatively stable species. Within the series of *p*-substituted aryls C_6H_4X, the rates of reductive elimination were remarkably little affected by the electron donating or withdrawing properties of X. Displacement of the pyridine donor of the C^N chelate ligand by a second equivalent of L proved essential in order to provide the conformational flexibility necessary for facile C-C bond formation; elimination here therefore takes place from a four-coordinate transition state $[(Ar^1)(Ar^2)AuL_2]^+$. C^N^{pz}^C pyrazine complexes reacted significantly faster than their pyridine analogues, likely reflecting the weaker coordination of pyrazine. Computational modelling showed that in gold(III)-C_6F_5 complexes pyridine displacement is comparatively facile but this is compensated by a higher barrier to C-C elimination, which explains the experimental finding of slow Ar-C_6F_5 coupling. By contrast, vinyl-aryl cross-coupling reactions proved to be fast even at -52 °C. The rates of aryl-R C-C cross-couplings decrease in the sequence *k*(vinyl) > *k*(aryl) >> *k*(C_6F_5) > *k*(Me). Phosphines induce faster reductive elimination than SMe_2, for both energetic and steric reasons, although their action is complicated by *cis/trans* isomerization. Modelling also suggests that in non-chelating systems three-coordinate species, $[(Ar^1)(Ar^2)Au(L)]^+$, *if formed*, would eliminate instantaneously, underlining the potential of gold(III) catalysts in smooth C-C bond forming reactions.

Acknowledgements

This work was supported by the European Research Council. M.B. is an ERC Advanced Investigator Award holder (grant no. 338944-GOCAT).

Supporting Information

Supporting information including synthetic procedures, NMR spectra and computational details can be found under http://dx.doi.org/10.1002/chem.201801277.

Keywords: gold • reaction mechanism • coupling reaction • reductive elimination • DFT calculations

[1] For recent reviews see for example: (a) A. S. K. Hashmi, G. J. Hutchings, *Angew. Chem. Int. Ed*. **2006**, *45*, 7896 – 7936. (b) L.-P. Liu, G. B. Hammond, *Chem. Soc. Rev.* **2012**, *41*, 3129–3139. (c) H. Schmidbaur, H. G. Raubenheimer, L. Dobrzanska, *Chem. Soc. Rev.* **2014**, *43*, 345-380. (d) R. Dorel, A. M. Echavarren, *Chem. Rev*. **2015**, *115*, 9028−9072. (e) J. Gil-Rubio, J. Vicente, *Dalton Trans*. **2015**, *44*, 19432–19442. (f) D.-A. Roşca, J. A. Wright, M. Bochmann, *Dalton Trans*. **2015**, *44*, 20785–20807. (g) M. N. Hopkinson, A. Tlahuext-Aca, F. Glorius, *Acc. Chem. Res*. **2016**, *49*, 2261−2272. (h) A. M. Asiria, A. Stephen K. Hashmi, *Chem. Soc. Rev.* **2016**, *45*, 4471-4503. (i) D. P. Day, P. W. H. Chan, *Adv. Synth. Catal*. **2016**, *358*, 1368 – 1384. (j) W.-W. Zi, F. D. Toste, *Chem. Soc. Rev.,* **2016**, *45*, 4567-4589. (k) J. Miró, C. del Pozo, *Chem. Rev*. **2016**, *116*, 11924−11966. (l) D. Pflästerer, A. S. K. Hashmi, *Chem. Soc. Rev.,* **2016**, *45*, 1331-1367. (m) R. J. Harris, R. A. Widenhoefer, *Chem. Soc. Rev.* **2016**, *45*, 4533—4551.

[2] M. Joost, A. Amgoune, D. Bourissou, *Angew. Chem. Int. Ed*. **2015**, *54*, 15022 – 15045.

[3] A. Tamaki, S. A. Magennis, J. K. Kochi, *J. Am. Chem. Soc*. **1974**, *96*, 6140-6148. (b) S. Komiya, T. A. Albright, R. Hoffmann, J. K. Kochi, *J. Am. Chem. Soc* **1976**, *98*, 7255-7265.

[4] S. Komiya, J. C. Huffman, J K, Kochi, *Inorg. Chem*. **1977**, *16*, 2138-2140.

[5] (a) C. F. Shaw III, J. W. Lundeen, R. S. Tobias, *J. Organomet. Chem*. **1973**, *51*, 365-374. (b) P. L. Kuch, R. S. Tobias, *J. Organomet. Chem.* **1976***, 122*, 429-446.

[6] A. Nijamudheen, S. Karmakar, A. Datta, *Chem. Eur. J.* **2014**, *20*, 14650 –14658.

[7] D. M. Kaphan, M. D. Levin, R. G. Bergman, K. N. Raymond, F. D. Toste, *Science* **2015**, *350*, 1235-1238.

[8] (a) J. Vicente, M. D. Bermúdez, J. Escribano, M. P. Carrillo, P. G. Jones, *J. Chem. Soc., Dalton Trans.* **1990**, 3083-3089. (b) J. Vicente, M. D. Bermúdez, J. Escribano, *Organometallics* **1991**, *10*, 3380-3384. (c) J. Vicente, M. D. Bermúdez, F. J. Carrion, *Inorg. Chim. Acta* **1994**, *220*, 1.

[9] Q. Wu, C. L. Du, Y. M. Huang, X. G. Liu, Z. Long, F. J. Song, J. S. You, *Chem. Sci*. **2015**, *6*, 288–293.

[10] R. Usón, A. Laguna, M. L. Arrese, *Synth. React. Inorg. Met.-Org. Chem*. **1984**, *14*, 557-567.

[11] M. Contel, A. J. Edwards, J. Garrido, M. B. Hursthouse, M. Laguna, R. Terroba, *J. Organomet. Chem*. **2000**, *607*, 129-136.

[12] (a) L. T. Ball, G. C. Lloyd-Jones, C. A. Russell, *Science* **2012**, *337*, 1644-1648. (b) L. T. Ball, G. C. Lloyd-Jones, C. A. Russell, *J. Am. Chem. Soc*. **2014**, *136*, 254−264.

[13] M. Hofer, E. Gomez-Bengoa, C. Nevado, *Organometallics* **2014**, *33*, 1328−1332.

[14] M. Hofer, A. Genoux, R. Kumar, C. Nevado, *Angew. Chem. Int. Ed.* **2017**, *56*, 1021 –1025.

[15] K. Kang, S. S. Liu, T. Xu, D. Wang, X. B. Leng, R. P. Bai, Y. Lan, and Q. L. Shen, *Organometallics* **2017**, *36*, 4727−4740.

[16] (a) Winston, M. S.; Wolf, W. J.; Toste, F. D. *J. Am. Chem. Soc*. **2014**, *136*, 7777-7782. (b) M. S. Winston, W. J. Wolf, F. D. Toste, *J. Am. Chem. Soc*. **2015**, *137*, 7921−7928.

[17] W. J. Wolf, M. S. Winston, F. D. Toste, *Nat. Chem*. **2014**, *6*, 159-164.

[18] K.-H. Wong, K.-K. Cheung, M. C.-W. Chan, C.-M. Che, *Organometallics* **1998**, *17*, 3505–3511.

[19] Review: R, Kumar, C. Nevado, *Angew. Chem. Int. Ed*. **2017**, *56*, 1994 – 2015.

[20] D.-A. Roşca, D. A. Smith, M. Bochmann, *Chem. Commun*. **2012**, *48*, 7247 – 7249, and cited references.

[21] J. Fernandez-Cestau, B. Bertrand, A. Pintus, M. Bochmann, *Organometallics*, **2017**, *36*, 3304–3312.

[22] D. A. Smith, D.-A. Roşca, M. Bochmann, *Organometallics* **2012**, *31*, 5988 - 6000.

[23] L. Rocchigiani, J. Fernandez-Cestau, P.H.M. Budzelaar, M. Bochmann, *Chem. Commun*., **2017**, *53*, 4358 – 4361.

[24] S. J. Lancaster, A. Rodriguez, A. Lara-Sanchez, M. D. Hannant, D. A. Walker, D. L. Hughes, M. Bochmann, *Organometallics* **2002**, *21*, 451-453.

[25] (a) B. R. Steele, K. Vrieze, Transition Metal Chem. 1977, 2, 140-144. (b) G. Alibrandi, G. Bruno, S. Lanza, D. Minniti, R. Romeo, M. L. Tobe, *Inorg. Chem.* **1987**, *26*, 185-190.

[26] H. J. Soscún Machado, A. Hincliffe, *J. Mol. Struct. (Theochem)* **1995**, *339*, 255-258.

[27] J. Fernandez-Cestau, B. Bertrand, M. Blaya, G. A. Jones, T. J. Penfold, M. Bochmann, *Chem. Commun*. **2015**, *51*, 16629 – 16632.

[28] M. J. Frisch, G. W. Trucks, H. B. Schlegel, G. E. Scuseria, J. R. Cheeseman, G. Scalmani, V. Barone, B. Mennucci, G. A. Petersson, H. Nakatsuji, M. Caricato, X. Li, H. P. Hratchian, A. F. Izmaylov, J. Bloino, G. Zheng, J. L. Sonnenberg, M. Hada, M. Ehara, K. Toyota, R. Fukuda, J. Hasegawa, M. Ishida, T. Nakajima, Y. Honda, O. Kitao, H. Nakai, T. Vreven, J. A. J. Montgomery, J. E. Peralta, F. Ogliaro, M. Bearpark, J. J. Heyd, E. Brothers, K. N. Kudin, V. N. Staroverov, R. Kobayashi, J. Normand, K. Raghavachari, A. Rendell, J. C. Burant, S. S. Iyengar, J. Tomasi, M. Cossi, N. Rega, J. M. Millam, M. Klene, J. E. Knox, J. B. Cross, V. Bakken, C. Adamo, J. Jaramillo, R. Gomperts, R. E. Stratmann, O. Yazyev, A. J. Austin, R. Cammi, C. Pomelli, J. W. Ochterski, R. L. Martin, K. Morukuma, V. G. Zakrzewski, G. A. Voth, P. Salvador, J. J. Dannenberg, S. Dapprich, A. D. Daniels, O. Farkas, J. B. Foresman, J. V. Ortiz, J. Ciolowski, D. J. Fox, B.01 ed., Gaussian, Inc., Wallingford CT, **2009**.

[29] (a) A. D. Becke, *J. Chem. Phys.* **1993**, *98*, 5648-5652; (b) A. D. Becke, *J. Chem. Phys.* **1993**, *98*, 1372-1377; (c) C. T. Lee, W. T. Yang, R. G. Parr, *Phys. Rev. B* **1988**, *37*, 785-789.

[30] A. Schäfer, H. Horn, R. Ahlrichs, *J. Chem. Phys.* **1992**, *97*, 2571-2577.

[31] P. J. Hay, W. R. Wadt, *J. Chem. Phys.* **1985**, *82*, 299-310.

[32] (a) S. Miertus, J. Tomasi, *Chem. Phys.* **1982**, *65*, 239-245; (b) S. Miertus, E. Scrocco, J. Tomasi, *Chem. Phys.* **1981**, *55*, 117-129; (c) G. Scalmani, M. J. Frisch, *J. Chem. Phys.* **2010**, 132.

[33] J. M. Tao, J. P. Perdew, V. N. Staroverov, G. E. Scuseria, *Phys. Rev. Lett.* **2003**, *91*, 146401.

[34] (a) T. H. Dunning, *J. Chem. Phys.* **1989**, *90*, 1007-1023; (b) D. E. Woon, T. H. Dunning, *J. Chem. Phys.* **1993**, *98*, 1358-1371.

[35] (a) Figgen, D.; Rauhut, G.; Dolg, M.; Stoll, H., *Chem. Phys.* **2005**, *311*, 227-244; (b) K. A. Peterson, C. Puzzarini, *Theor. Chem. Acc.* **2005**, *114*, 283-296.

[36] S. Grimme, J. Antony, S. Ehrlich, H. Krieg, *J. Chem. Phys.* **2010**, *132*, 154104.

[37] S. Kozuch, S. Shaik, *Acc. Chem. Res*. **2011**, *44*, 101-110.

10.1002/chem.201801277

WILEY-VCH

Entry for the Table of Contents

FULL PAPER

Protolytic Au-C bond cleavage of (C^N^C)AuR pincer complexes, followed by addition of ≥2 equivalents of SMe_2 leads to reductive aryl-R elimination, with rates decreasing in the sequence *k*(vinyl) > *k*(aryl) >> *k*(C_6F_5) > *k*(Me). Vinyl-aryl coupling is very fast even at -52 °C.

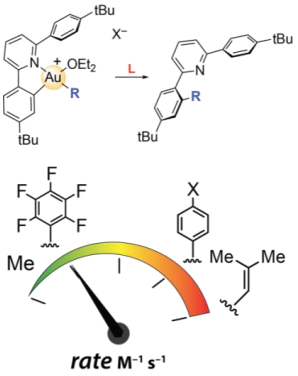

Luca Rocchigiani, Julio-Fernandez-Cestau, Peter H. M. Budzelaar* and Manfred Bochmann**

Page No. – Page No.

Reductive Elimination Leading to C-C Bond Formation in Gold(III) Complexes: A Mechanistic and Computational Study